International Conference
Nuclear Energy for New Europe 2005
Bled, Slovenia, September 5-8, 2005

Flow in Rod Bundles

Gábor Házi, Gusztáv Mayer
KFKI Atomic Energy Research Institute
H-1525, Budapest, Hungary
gah@sunserv.kfki.hu, mayer@sunserv.kfki.hu

ABSTRACT

For power upgrading VVER-440 reactors we need to know exactly how the temperature measured by the thermocouples is related to the average outlet temperature of the fuel assemblies. Accordingly, detailed knowledge on mixing process in the rod bundles and in the fuel assembly head have great importance. Here we study the hydrodynamics of rod bundles based on the results of direct numerical and large eddy simulation of flows in subchannels. It is shown that secondary flow and flow pulsation phenomena can be observed using both methodologies. Some consequences of these observations are briefly discussed.

1 INTRODUCTION

In VVER-440 reactors the thermocouples are positioned in the head of the fuel assembly about 50 cm above the fuel rod bundle. It was believed that the coolant is well mixed at that position and accordingly it was assumed that the thermocouples detect some kind of average temperature of the outlet fuel temperature. Recent numerical calculations using computational fluid dynamics (CFD) tools have not supported that assumption. Since, the value of the outlet temperature is related to fuel limit parameters, the power upgrading plans of VVER-440 reactors motivated us to obtain more information on the mixing process of the fuel assemblies.

In a recent note [1] it has been demonstrated that the simulation of rod bundle flows is not a trivial task using commercial CFD. Attention has to be paid to the turbulence model selection, since rod bundle flows are more complex than simple channel flows.

Most of our current knowledge on rod bundle flows is due to experimental observations. The first measurements had been carried out in the early seventies but, as a result of the development of the measurement techniques additional key observations were presented in the late nineties [2-7]. An early observation is that the turbulent flow in a rod bundles and in pipes have different characteristics (for details see e.g. [5] and references therein). As a consequence, the classical engineering approach, which tries to trace the characterization of such systems back to equivalent pipe flows, does not give reasonable results. Due to the different turbulence characteristics, the mixing is more intensive in rod bundles than it would be expected based on equivalent pipe flow correlations. At present, there are two basic hypotheses for the explanation of the high mixing.

As a possible explanation, secondary flow was deduced from measurements by several experimentalists [2,3,5,6] and quite recently its existence has been supported by analytical

results [8]. In rod bundles the secondary flow appears as circulation in the elementary cells of the subchannels, at least in a statistical sense. It means that taking a longtime average of the lateral velocity components, the mean velocities show a macroscopic circulation. In the neighboring cells the rotation has opposite directions.

Another candidate to explain the high mixing is the so-called flow pulsation phenomena. The velocity component along the rods has a maximum in the gap regions, again in a mean sense. It has been observed in the recent experiment of Krauss and Meyer [5] that the flow oscillates in this region. Vortices are transported in the longitudinal direction more or less periodically with this oscillating flow. The interactions between the transported vortices result in a gain in the momentum transfer i.e. increase the mixing.

In this paper we present subchannel simulations using direct numerical and large eddy simulation methodologies. These approaches are briefly reviewed in Section 2. As a numerical solver we use a lattice Boltzmann model, which is briefly introduced in Section 3. Section 4 is dedicated to specify the problem to be solved. In Section 5 the results of the simulations are presented. Finally, conclusions are drawn in Section 6.

2 DIRECT NUMERICAL AND LARGE EDDY SIMULATION

The simulation of turbulent flow is difficult, basically because the spectrum of the relevant length scales is wide. One has to resolve all the scales accurately unless some turbulence model is used considering the effect of the unresolved scales on the resolved ones. Resolving all the relevant scales of the turbulent flow means the direct numerical simulation of the problem. The wide spectrum of the relevant scales is a consequence of the nonlinear term in the momentum conservation equation. The Reynolds number ($\mathrm{Re} = uL/\nu$ where u is the characteristic velocity, L is the characteristic length and ν is the kinematic viscosity) gives an indication how the nonlinear terms are related to the viscous dissipative ones. When the Reynolds number is in the order of 1, the inertial and viscous forces are close to balance. Numerical experiments show that in direct numerical simulation the numerical grid has to be fine enough to have a cell Reynolds number $\mathrm{Re}_d = ud/\nu \cong O(1)$, where d is the grid spacing [10]. If the characteristic length is in the order of the length of the physical domain, which is often the case, then a rough estimation shows that the required number of cells scales with the Reynolds number. Therefore high Reynolds number flows can not be studied by direct numerical simulation. In spite of this fact, the direct numerical simulation can be used to study turbulent flows and being a modeless approach, it might provide invaluable information on such flows.

Large eddy simulation is a good candidate to study time dependent high Reynolds number turbulent flows. The basic idea behind the large eddy simulation is to resolve the large scales accurately and model the small scales by simple models. There are both experimental and theoretical evidences that in high Reynolds number turbulent flows the small scales have universal characteristics in contrast to the large scales, which behave problem dependent. The basic problem with the Reynolds-averaged Navier-Stokes approach used in commercial CFD codes that it requires models for all the scales. After more than one century research one can say with high confidence that it is very difficult to work out such a model. On the contrary, using large eddy simulation we need model only for the universal small scales and accordingly, simple models can work pretty well. It is worth mentioning that: still we need to resolve a very wide range of scales accurately, which is often challenging from computational point of view. Increasing the resolution of a large eddy simulation and correspondingly increasing the number of the resolved scales, the role of the turbulence model decreases. A kind of limit of large eddy simulation is the direct numerical simulation, where,

as we have seen, all the relevant scales are resolved and we do not need turbulence model anymore.

More details about direct numerical simulation and large eddy simulation can be found in [9,10] or in textbooks, see e.g. Section 9 in the recent edition of Ferziger and Peric [11].

3 THE LATTICE BOLTZMANN METHOD FOR DIRECT NUMERICAL AND LARGE EDDY SIMULATION

Recently, the lattice Boltzmann method (LBM) has been developed as a new innovative numerical method for fluid flows based on kinetic theory. For a review see e.g. [12]. This method can be viewed as a simple Navier-Stokes solver and can be adopted for direct and large eddy simulation of single phase turbulent fluid flow. Here we briefly review the numerical model we applied for our simulations.

Using LBM a lattice - having sufficient symmetry - is laid on the geometrical domain and the following evolution equation for the one-particle velocity distribution functions is solved:

$$f_i(\mathbf{r}+\mathbf{c}_i\Delta t, t+\Delta t) - f_i(\mathbf{r},t) = \Omega(f_i), \tag{1}$$

where ***c(r,t)*** is the particle velocity and ***f(r,c,t)*** is defined such that ***f(r,c,t)drdc*** is the number of molecules at time *t* positioned between ***r*** and ***r***+***dr*** which have velocities in the range ***c*** and ***c***+***dc*** and the index *i* is used to identify the lattice links.

In our simulations we used a D3Q27 model, so the lattice vectors are specified as follows:

$$\mathbf{c}_i = \begin{pmatrix} (0,0,0) & \text{if } i=0 \\ (\pm 1,0,0),(0,\pm 1,0),(0,0,\pm 1) & \text{if } i=1,2,...,6 \\ (\pm 1,\pm 1,0),(\pm 1,0,\pm 1),(0,\pm 1,\pm 1) & \text{if } i=7,8,...,18 \\ (\pm 1,\pm 1,\pm 1,) & \text{if } i=19,20,...,26 \end{pmatrix}. \tag{2}$$

In eq. (1), Ω is a collision operator, which has the simplest so-called BGK form in our approach [13,14]:

$$\Omega_i = -\frac{1}{\tau}(f_i - f_{i,eq}), \tag{3}$$

where τ is a relaxation time and the equilibrium distribution function has the following form:

$$f_{i,eq}(\rho,\mathbf{u}) = \rho w_i\left[1+\frac{1}{c_s^2}(\mathbf{c}_i\cdot\mathbf{u})+\frac{1}{2c_s^4}(\mathbf{c}_i\cdot\mathbf{u})^2-\frac{1}{2c_s^2}u^2\right]. \tag{4}$$

The *w*'s in (4) are the weights of the links:

$$w_i = \begin{pmatrix} 8/27 & \text{if } i=0 \\ 2/27 & \text{if } i=1,2,...,6 \\ 1/54 & \text{if } i=7,8,...,18 \\ 1/216 & \text{if } i=19,20,...,26 \end{pmatrix}. \tag{5}$$

The macroscopic quantities like the density ρ and hydrodynamic velocity ***u*** can be obtained as the following moments of the distributions functions:

$$\rho = \sum_i f_i, \qquad \mathbf{u}\rho = \sum_i \mathbf{c}_i f_i. \tag{6}$$

It can be shown by a Chapman-Enskog expansion that these macroscopic quantities satisfy the Navier-Stokes equations up to second order both in time and space in the low Mach number limit:

$$\partial_t \rho + \nabla \cdot (\rho \mathbf{u}) = 0, \tag{7}$$
$$\partial_t (\rho \mathbf{u}) + \nabla \cdot (\rho \mathbf{u}\mathbf{u}) = -\nabla \cdot (\rho c_s^2) + \nabla \cdot \rho \nu \left(\nabla \mathbf{u} + (\nabla \mathbf{u})^t\right).$$

In Eq. (7) c_s is the speed of sound and ν is the kinematic viscosity of the fluid:

$$c_s = \sqrt{1/3}, \qquad \nu = \frac{1}{3}\left(\tau - \frac{1}{2}\right). \tag{8}$$

Note that the pressure is obtained by the simple equation of state:

$$p = c_s^2 \rho. \tag{9}$$

One of the major advantages of the lattice Boltzmann method is that the evolution equation (1) can be solved by a simple ‘streaming and collision’ procedure, which can be massively parallelized. The algorithm is as follows:

1. Move all distribution functions to the neighboring sites according to the direction of the lattice vector (streaming).
2. Apply the collision operator Eq. (3) to calculate the new values of *f*’s (collision).
3. Calculate the macroscopic quantities using Eq. (6). These quantities can be used in the next step to calculate the equilibrium distribution Eq. (4).
4. Go to 1.

No-slip boundary conditions were implemented using the interpolated bounce-back method, recently proposed by Yu et al. (2003).

The above approach can be used directly to solve the Navier-Stokes equation, so it can be used for the direct numerical simulation of turbulent flows. Although some doubts arose about the applicability of the LBM for direct numerical simulation [16], recent comparison of the simulation results of decaying two-dimensional homogenous, isotropic turbulence using the LBM and a pseudospectral method shown [17], that the LBM can provide highly accurate results for turbulent flows.

The LBM also can be used as a framework for large eddy simulation. Here we adopted the approach used in [18,19] with the simple Smagorinsky model. That is no explicit filtering was used and the subgrid scale stresses were obtained from the second moments of the distribution functions.

4 GEOMETRY OF THE SUBCHANNEL AND PROBLEM SPECIFICATION

In a VVER-440 type fuel rod bundle the rods are arranged in a triangular array. For the simulations we used a regular hexagonal prism around a rod inside the rod bundle as a computational domain. Each side of the computational domain was coupled periodically. In the longitudinal direction also periodic boundary conditions were applied and the flow was driven by a body force. It is worth noting that both the direct numerical and large eddy simulation is time dependent approach. Since in turbulent flows, the symmetries exist only in

a statistical sense therefore the symmetry planes of the subchannels can not be exploited. The application of periodic boundary conditions might be questionable, too. Only, the comparison between the simulation results and the measurements can prove that our computational domain is long enough and the application of the periodic boundary conditions does not influence the solutions significantly.

It has to be mentioned that our numerical mesh has regular cubes. Since using such mesh a perfect triangular arrangement can not be built up, therefore some symmetries break down in our domain. The asymmetry of the arrangement decreases as we increase the resolution i.e. the number of the grid points.

Our code was validated by comparing the simulation results with analytical solutions. As a reference the explicit solution for laminar flow along triangular array of rod bundles of Drummond and Tahir [20] was used. Using 104x104 cells in the lateral directions and 10 cells in the longitudinal direction we have found that the maximum relative error of the velocity is less than 1% in steady-state. The largest errors could be observed around the walls. The comparison proved that the implementation of the method is right and the high accuracy achieved supported the application of our numerical approach for direct numerical and large eddy simulations.

5 SIMULATION RESULTS

Several simulations have been carried out and here only a small subset is presented focusing on the most important results, which have practical relevancies.

5.1 Direct numerical simulation results

Direct numerical simulation has been carried out using a bounding box 208x240x206. Only the active fluid nodes were considered in the domain, which means roughly 4 million computational cells. Constant axial velocity was specified as an initial field with a small random perturbation in the pressure field. The body force was introduced and the fluid started to accelerate. Very rapidly a laminar profile developed, which lost its stability by the increasing velocity. As the turbulence had developed the momentum loss increased and the axial velocity decreased. Finally the axial velocity oscillated around a mean value more or less periodically. Based on the mean axial velocity the Reynolds number is around 4000. The time evolution of the velocity components at a certain point in the fluid domain is shown in Fig. 1 considering 400.000 steps. During this time interval one can see only a few oscillations in the domain. This oscillation can be associated with the flow pulsation phenomenon observed by Krauss and Meyer [5].

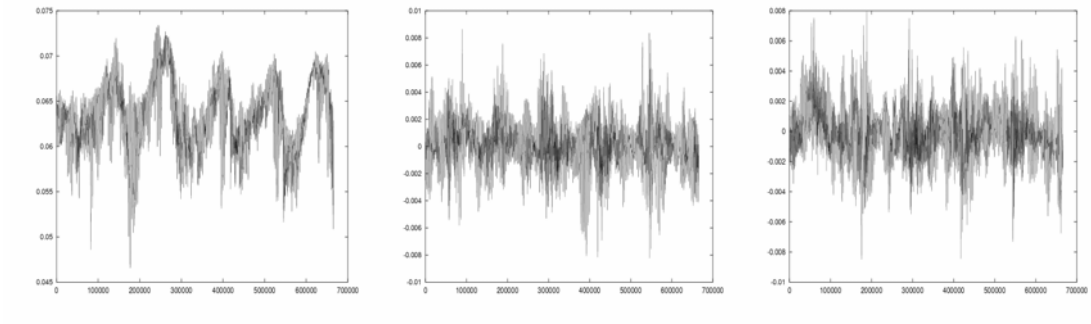

a. b. c.

Fig 1. Time evolution of the velocity components after the onset of turbulence (longitudinal component – (a), later components – (b,c)).

To get some qualitative picture about the flow two snapshots of the axial velocity are shown in Fig. 2. A “longtime” color movie of the same physical parameters can be found in our web page [21]. Some vortex detachment points can be clearly observed in the simulation results. These detachment points do not change their position significantly in the time interval considered. Most of these points can be assigned to the corners of the domain or with other words to the “gaps”. Although the position of the detachment points do not move, but the directions of the detachments oscillate, producing positive z vorticity component on one side of the detachment point and negative on the other side. Some detachment points, oscillating in somewhat less regular way, can not be assigned to gaps. They sometimes interact with the gap vortex sources and then disappear from the landscape. The overall effect of the flow oscillation is high mixing.

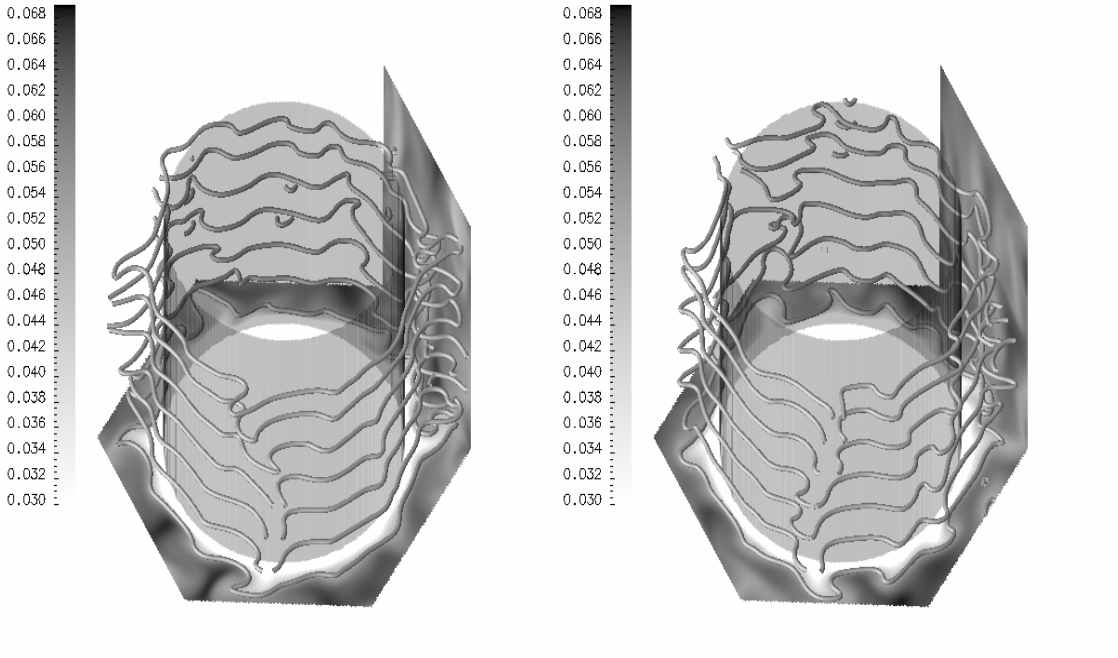

Fig. 2 The axial velocity profile at two time instants is shown using contour lines at different axial levels.

Considering secondary flow, it is interesting to see a time average of the axial velocity component and the projection of the mean lateral velocity components (Fig. 3).

Fig. 3 Contours of the mean axial velocity (left) and the projection of the mean lateral velocities to a cross section.

Because of the high computational cost, the average was taken considering only 7 periods of the oscillations. Looking at the contours of the mean axial velocity it seems that the

flow is still not settled down perfectly in a statistical sense during this time period, so the lack of symmetry might be a consequence of the insufficiently long averaging. In spite of this fact some secondary flow can be observed in some elementary cells of the subchannel (see the cells on the right) just as it is predicted from measurements.

Summarizing, the direct numerical simulation shows a quite simple picture on the flow in rod bundles. Both the flow pulsation phenomenon and the secondary flow could be identified as a source of high mixing in rod bundles. From the simulation results it seems that the two phenomena are not independent from each other, but we suspect that the development of the secondary flow is a consequence of the flow pulsation. Our suspicion is based on the visual observation of the flow [21]. It is worth noting that such observation can be done only at relatively low Reynolds number at which we have large enough structures to observe.

5.2 Large eddy simulation results

In order to study the flow at higher Reynolds numbers we carried out several simulations. In the simulation considered in this paper we used a bounding box 104x120x206. Again, only the active fluid nodes were considered in the domain, which means roughly 500.000 computational cells. The time evolution of the axial velocity at a certain point in the fluid domain is shown in Fig. 4. Here one can see the initial phase of the simulation and identify the onset of turbulence.

Flow pulsation also can be deduced from the later phase of the time evolution, although its appearance is less obvious from the figures. At this simulation the Reynolds number was about 25000. Fig. 5 shows some snapshots of the axial velocity. Comparing these results with that of the direct numerical simulation, much smaller structures appear in the simulation domain, which is due to the higher Reynolds number. It is difficult to identify a clear mechanism for vortex generation even from the movie, which is available again in our web site [21]. However, taking a long time average of the solution the results seems to be promising. The contours of the mean axial velocity can be seen in Fig. 6. The axial velocity shows a typical picture known from rod bundle measurements [5,6]. Considering the lateral velocities it is obvious that our simulation results still not respect all the symmetry properties of the channel. As we have mentioned we have some symmetry breaking due to the cubic mesh we used in our simulations, so the lack of perfect symmetry might be the consequence of that. It is worth noting that the magnitude of the lateral velocity is a few percent of the longitudinal velocity, again in line with measurements.

Considering the resolution used in this simulation, it would mean that a few micrometer displacement of rods can significantly influence the flow pattern development in rod bundles. This observation also implies a serious practical consequence. Since in industrial systems such displacement, rod vibration etc. are always present, the detailed knowledge of the nice regular arrangement might be needless. It is no use to know the exact flow pattern of the regular arrangement if in real systems the uncertainty of the geometry of the bundle results in something else.

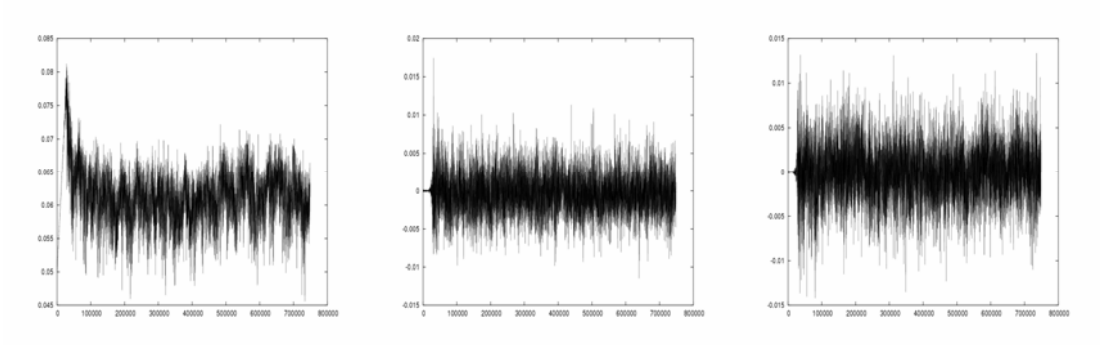

a. b. c.

Fig. 4 Time evolution of the axial (a) and lateral (b,c) velocities.

We should still not exclude another possible explanation, namely that the Reynolds number is relatively low in our simulation and it might influence the developing flow significantly. This possibility is also supported by some of our recent large eddy and CFD simulations using Reynolds-averaged Navier-Stokes approach with Reynolds-stress transport model. In those calculations the converged steady-state solution changed significantly by varying the body force acting on the fluid. Although the contours of the axial velocity in a cross section showed nice symmetric patterns, the lateral components behaved quite randomly. At low velocities they sometimes formed only a few circulation cells, not respecting the symmetry properties of the simulation domain at all. However, at sufficiently high Reynolds number we could observe all the circulation cells as it was expected. It is worth keeping in mind that the direct numerical simulation results also suggest some Reynolds number dependence.

The possibility of strong Reynolds number dependence has some practical relevance, since one of the next-generation nuclear reactors, namely the supercritical water cooled (SCW) reactor is planed to operate at much lower flow rate than the pressurized water reactors. Accordingly, the Reynolds number effect might be relevant, which should be taken into account during the design phase of the fuel rod assemblies of CSW reactors.

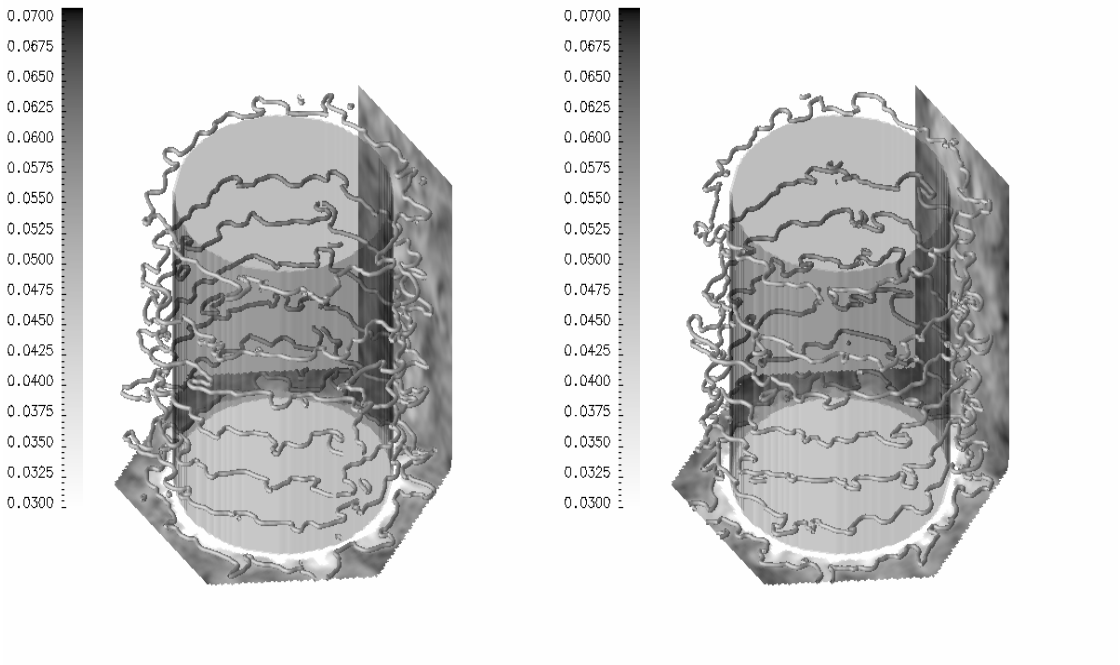

Fig. 5 Snapshots of the axial velocity.

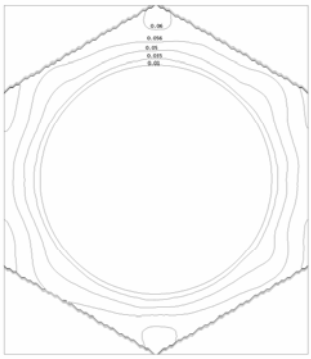

a.

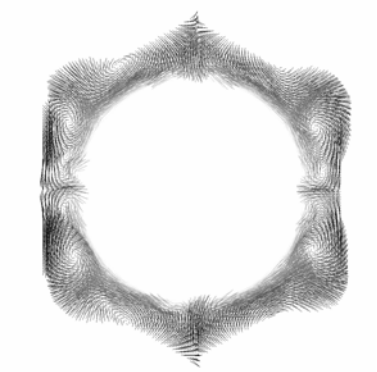

b.

Fig. 6 Contours of the mean axial velocity (a) and the projection of the mean lateral velocities (b) to a cross section.

6 CONCLUSION AND FUTURE PLANS

Simulation results of subchannels have been presented using the direct numerical and large eddy simulation approaches. The simulations have been carried out using a lattice Boltzmann framework. The flow pulsation phenomenon could be observed clearly in the direct numerical simulation results. Secondary flow patterns were observed using both methodologies. The time evolution of the flow can be seen in our web site [21]. The simulation results suggest that the development of the secondary flow patterns might depend on the Reynolds number and/or it might be very sensitive to small rod displacement. Further investigations are needed before drawing a definite conclusion. Accordingly, PIV measurements will be carried out in our institute at various Reynolds number and the simulation studies will be extended in many respects (length of the channel, Reynolds number range etc.). A more detailed analysis of the simulation results (including Reynolds stresses etc.) will be presented in some fluid mechanical journal.

REFERENCES

[1] Házi, G., 2005, On Turbulence Models for Rod Bundle Flow Computations, *Annals of Nuclear Energy*, 32, pp. 755

[2] Seale W.J., 1979, Turbulent Diffusion of Heat between Connected Flow Passages, *Nucl. Eng. Des.*, 54, pp.183

[3] Rehme K., 1987, The Structure of Turbulent Flow through Rod Bundles, *Nucl. Eng. Des.*, 99, pp. 141

[4] Rehme K., 1973, Simple Method of Predicting Friction Factors of Turbulent Flow in Non-circular Channels, *Int. J. Heat Mass Transfer*, 16, pp.933

[5] Krauss T., Meyer L., 1998, Experimental Investigation of Turbulent Transport of Momentum and Energy in Heated Rod Bundle, *Nucl. Eng. Des.*, 180, pp.185

[6] Trupp A.C., Azad R.S., 1975, The structure of turbulent flow in triangular array rod bundles, *Nucl. Eng. Des.*, 32, pp. 47

[7] Trippe G., Weinberg D., 1979, Non-isotropic Eddy Viscosities in Turbulent Flow through Rod Bundles, *Turbulent Forced Convection in Channels and Bundles,* Ed. Kakac S., Spalding D.B. Hemisphere Publ. Corp. Washington, Vol. 1, pp. 505

[8] Kim S., Kim M.C., 2004, A Note on the Azimuthal Momentum Transport in Infinitely Arrayed Rod Bundles, *Int. Comm. Heat Mass Transfer*, 31, pp. 333

[9] Rogallo R.S., Moin P., 1984, Numerical Simulation of Turbulent Flows, *Ann. Rev. Fluid Mech.*, 16, pp. 99

[10] Moin P., Mahesh K., 1998, Direct Numerical Simulation: A Tool in Turbulence Research, *Ann. Rev. Fluid Mech.*, 30, pp. 539

[11] Ferziger J.H., Peric M., 2002, Computation Methods for Fluid Dynamics, *Springer-Verlag, Berlin*

[12] Házi, G., Imre A.R., Mayer G., Farkas I., 2002, Lattice Boltzmann Methods for Two-phase Flow Modeling, *Annals of Nuclear Energy*, 29, pp. 1421

[13] Qian Y.H., d'Humiéres, Lallemand P., 1992, Lattice BGK models for Navier-Stokes equation, Europhys. Letters, 17, pp. 479

[14] Bhatnagar P. L., Gross E. P., Krook M., 1954, A Model for Collision Processes in Gases. I. Small Amplitude Processes in Charged and Neutral One-Component Systems, *Phys. Rev.*, 94, pp. 511

[15] Yu D. Luo M.R., Shyy W., 2003, Viscous flow computations with the method of lattice Boltzmann equation, *Prog. Aerospace Sci.*, 39, pp. 329

[16] Házi, G., 2005, Bias in the Direct Numerical Simulation of Isotropic Turbulence Using the Lattice Boltzmann Method, *Phys. Rev. E,* 71, pp. 036705

[17] Házi, G., Jiménez C., 2005, Simulation of two-dimensional decaying turbulence using the “incompressible” extensions of the lattice Boltzmann method, Comp. Fluids, in press

[18] Hou S., Sterling J., Chen S., Doolen G.D., 1996, A Lattice-Boltzmann subgrid model for high Reynolds number flows, *Fields Instr. Comm.*, 6, pp. 151

[19] Treeck C., Krafczyk M., Kühner S., Rank E., (2001) Direct Building Energy Simulation Based on Large Eddy Techniques and Lattice Boltzmann Methods, *VII. Int. IBPSA Conference*, Rio de Janeiro, Brazil, Aug. 13-15

[20] Drummond J.E., Tahir M.I., 1984, Laminar Viscous Flow through Regular Arrays of Parallel Solid Cylinders, *Int. J., Multiphase Flow*, 10, pp. 515

[21] Mayer G., Házi G., 2005, www.kfki.hu/~aekiszl